Full Length Research Paper

The solar-reflective characterization of solid opaque materials

Thomas Allmendinger

Glattbrugg/Zurich, Switzerland.

With respect to the reflective behaviour of solar radiation on solid surfaces being relevant for (micro)-climate modelling, particularly at pavements, buildings and roofs, it is proposed that making a difference between the colour dependent terms albedo a_s and solar reflection coefficient α_s, the former being related to a white surface and the latter being related to the total incident solar radiation. As a complement to the solar reflection coefficient, the solar absorption coefficient $\beta_s = 1 - \alpha_s$ is defined. For conceiving the thermal behaviour of solid materials in the presence of sunlight, a novel method is described for directly determining the solar absorption coefficient, instead of the usual but delicate methods where the incident and the reflected radiation are measured delivering the solar reflection coefficient. Thereto, the heat absorbance rate of coloured solid plates is determined by measuring their temperatures, and regarding their heat capacities. Since the warming-up process is interfered by a heat emission, the cooling down behaviour has to be known. Thereto, separate measurements were made with preheated plates in a darkened room, the obtained results differing from the forecast by the widely used Stefan-Boltzmann law. For both processes, mathematic modelling was derived enabling an arithmetic combination of the warming-up and the cooling-down process yielding limiting temperatures being solely dependent on the surface colour. Finally, some comparing albedo-measurements were made using a normal light-meter being directed towards wooden boards which have been coloured the same as the original plates, yielding a remarkably good accordance of the two methods.

Key words: Albedo, radiation-absorption, heat-emission, Stefan-Boltzmann law, climate-modelling.

INTRODUCTION

For climate modelling, the so called »albedo« plays an important part. In particular, it explains the so called urban heat island effect. The term is derived from Latin meaning "whiteness", and was introduced by Johann Heinrich Lambert in his 1760 work "Photometria", being commonly assumed as the colour-dependent solar reflection coefficient, normally indicated by α, concerning solar light and expressing the intensity-ratio of light being reflected by a surface compared to the incident light. A bright surface exhibits a high albedo that which is

E-mail: inventor@sunrise.ch.

tantamount to a high portion of reflected light. Logically, the highest possible value of the albedo is 1.

But already with the definition of the term »albedo« some ambiguities arise, for, strictly speaking and regarding its true meaning, the albedo value should not be an absolute one but a relative one, namely being related to a white surface. However, in the literature such a distinction is not made. Rather, the terms "albedo" and "solar reflection coefficient" are used as synonyms. Moreover, according to the citations in the publication of Coulson and Reynolds (1971), one finds the apparent synonyms "spectral reflectance", "optical reflection", "reflection of direct radiation" and "reflectivity".

A further intricacy is given by the fact that actually not the reflection of the light is relevant for thermal changes of the solid earth surface, or of their artificial modifications such as buildings, but the absorption, hence in climate modelling indeed the solar absorption coefficient (here named β_s) is used and not the solar reflection coefficient (here named α_s). Arithmetically, the two terms are complementary: $\beta_s = 1 - \alpha_s$. However, physically there is a principal difference insofar as the absorbed energy is of another type than the reflected one: the first one affects partly heat, while the second one affects only radiation power. Moreover, as a result of this reflection the radiation is transformed and scattered, changing its character and its colour, since this kind of reflection is not the same as a reflection of light on a mirror surface. And furthermore, both energies may engender subsequent implications, in particular warming-up the adjacent atmosphere. Therefore, the aforementioned equation is not such trivial as it appears prima facie.

This fact is insofar relevant as normally the reflection coefficient is determined, and not the absorption coefficient. That's because for the field measurements being originally made, concerning landscapes or cities, the former method is easier to carry out but still exhibiting several difficulties. For example, field-measurements of the optical reflection characteristics of various natural sands and soils at different wavelengths by Coulson et al. (1965) showed that there is a strong dependency of the intensity and degree of polarization of the reflected radiation on the angle of the incident radiation, particularly at longer wavelengths. Similar dependencies were also found for various other surfaces, soils and types of vegetation (Coulson and Reynolds, 1971; Nkemdirim, 1972).

Normally, the solar reflection coefficient is determined by "albedometers" where the intensities of incident solar light, on one hand, and of reflected light, on the other hand, are compared. A principal description is given in the ASTM Standard E1918-06. Therein, the light intensity is simultaneously measured by two diametrically opposed »pyranometers«, being approx. adapted to the electromagnetic spectrum of solar light extending from wavelength 300 to 3500 nm, where the range <380 nm matches UV (ultraviolet) radiation, and the range >760 nm matches IR (infrared) radiation. In the earlier mentioned standard specification, a pyranometer operating in the range of 280 to 2800 nm is recommended. Thereby, it is worth knowing that the entire infrared range extends up to much longer wavelengths, also comprising the thermal radiation of solids describable by Planck's law (according to which the intensity peak e.g. at 300 K is in the region of 10'000 nm = 10 µm), while here only the short wavelength range of IR (also called NIR = near IR) is involved. However, the aforementioned special character of the reflected light leads to several inherent measuring problems being originally described by Coulson (1975) and later by Zerlaut (1989). The state of the art, comprising subsequent improvements, is outlined by Levinson et al. (2010).

An alternative, more sophisticated approach for describing the reflection behaviour of pigments is based on spectroscopic measurements on transparent films, focussing the near-infrared range of the irradiance. Thereby, the reflectance and the transmittance of a freely suspended transparent film, being coated with a pigment, are detected.

A comprehensive description of this method, being established by several authors, as well as some specific results, is given by Levinson et al. (2005). It starts from the feature of the North-American solar irradiance spectrum (300 to 2500 nm) that visible light (400 to 700 nm) accounts for only 43% of the energy in the air-mass, while the remainder arrives as near-infrared (700 to 2500 nm, 52%) or ultraviolet (300 to 400 nm, 5%) radiation. The intention of the relating philosophy is to improve preferentially the reflection-power in the NIR-range of radiation, and not the one in the visible range, thus creating dark pigments with a high albedo. This wondrous inversion is aptly expressed by the title of a publication of Brady et al. (1992) in a commercial magazine: "When black is white." However, with respect to the practical relevance of its results, this method has to be queried since a direct coherence to coloured solid opaque materials is not given, and a calculation of the heat absorbance degree is not possible. Moreover, the assessment of the empirical results affords a quite complicated theory exhibiting a variety of parameters, while comparing measurements on base of a different method are missing.

In reality, the circumstances are even more complex since the surface material overtime grows warm giving off heat to the atmosphere, be it by radiative emission, or be it by conductive heat transfer. Hence, the transformative reflection of solar light is superimposed by an emission of heat.

For theoretically describing the temperature dependent radiative emission of a solid surface, usually the formula of Stefan (1879) and Boltzmann (1884) is applied, expanded by the "spectral emissivity" ε (cf. Visconti, 2001, p. 8), and delivering a value for the limiting surface temperature T_{lim} in the presence of vertically incident solar radiation:

$$S * \cdot \beta_s = \varepsilon \cdot \sigma(T_{\lim}^4 - T_{air}^4) \tag{1}$$

where $S* =$ solar-constant at the Earth surface (= terrestrial solar-constant), β_s = solar absorption-coefficient = $1 - \alpha_s$, ε = spectral emissivity, and σ = currently assumed Stefan-Boltzmann-constant = $5.67 \cdot 10^{-8}$ Wm^{-2}K^{-4}

The forth power of the absolute temperatures at ordinary temperature conditions near the Earth surface may be substituted by the simple first power expression:

$$T_1^4 - T_2^4 \cong 4T_2^3\left(T_1 - T_2\right) \tag{2}$$

where the factor $4\sigma \cdot T_2^3$ becomes theoretically approximately 6 Wm^{-2}K^{-1} when $T_2 = 300$ K (cf. Meschede, 2002: 236).

Actually, Stefan's approach – being deduced from ancient measurements of Dulong and Petit (1817) - supposes a radiation and a back-radiation. However, apart from the peculiar spectral emissivity term, this formula exhibits a raw point by assuming that the two radiation sources are of similar type, namely black bodies. But it seems quite unlikely assuming the atmosphere as a black body. Moreover, the formula comprehends no distance term for the two sources. Therefore, it appears advisable empirically checking the validity of that formula, comparing it with the Newton law (3), resembling Equation 2 but exhibiting another factor B named heat transfer coefficient [Wm^{-2}K^{-1}]:

$$S * \cdot \beta_s = B(T_{\lim} - T_{air}) \tag{3}$$

One of the first practical material specific information is 1963 given by J. F. Black regarding asphalt pavements. More than 30 years later, but referring to a previous paper of Johnson and Watson (1984), Asaeda et al. (1996) observed and analysed the heat flux at the air/ground interface for various pavement materials on summer days. The surface temperature, heat storage and its subsequent emission to the atmosphere were significantly greater for asphalt than for concrete or bare soil. At the maximum, asphalt pavement emitted an additional 150 Wm^{-2} in infrared radiation and 200 Wm^{-2} in sensible transport compared to bare soil surface. Analyses of the atmosphere indicated that most of the infrared long wave radiation from the ground was absorbed within 200 m of the lower atmosphere affecting air temperature near the ground. With large difference between air and ground surface temperature at noon, the rate of infrared absorption by the lower atmosphere over asphalt pavement was greater by 60 Wm^{-2} than that over the soil surface or concrete pavement.

With the objective of reducing the demand of air-conditioning costs in warm places by reducing the interior temperature of buildings, Pomerantz et al. (1999) made temperature measurements with twelve 10 cm square pavement-samples in an array being attached to an insulating foam board which had been covered with an unpainted cotton artist's canvas. Underneath each sample, a thermocouple was placed. The sample board was placed on a wooden roof platform only 10 cm above the roof surface and tilted up to face the midday sun (zenith angle, 55°). The wind conditions were "breezy enough to move papers around but less than a stiff wind", hence quite undefined. No on-site wind measurements were performed though it was conceded that the effect of convection were quite evident. The temperature rise was measured relative to the local air temperature.

Each sample attained its maximum or stagnation temperature after a few minutes in the sun. Thereafter, the sample temperatures fluctuated erratically, by several degrees, as gusts of wind come and go. The relevant heat emission of the samples was not measured but solely calculated, using the Stefan-Boltzmann relation. Possible distortions, particularly of the wind, have not been quantitatively incorporated or minimized, thus an analytical consideration delivering material specific values is not feasible.

Doulos et al. (2004) and Synnefa et al. (2006, 2007) studied different building materials recording the mean hourly ambient temperature during the day as well as during the night, and using sampling tiles with a normal size of 40 × 40 cm. The sampling tiles were placed on an especially modulated platform covering a surface of 40 m^2, but being not embedded within a heat-isolating material such as Styrofoam, and being not orientated in a well-defined direction. The selected sample materials consisted of several different construction materials, of different surface colour materials, and of different surface texture materials. The basic experimental equipment used for the implementation of the measurements consisted of an infrared camera to measure surface temperatures. Measurements were also performed by using contact thermometers in order to take into account minor errors associated with reflected infrared radiation and the non-complete knowledge of the material emissivity. The optical and thermal criteria were both regarded but not separated, so the classification »cold materials« were vaguely characterized by a high reflectivity factor to the short-wave radiation and a high emissivity factor to the long-wave radiations. Within the study published in 2006, an infrared camera was used in order to observe the temperature distribution on the surface of the samples as well as to depict the temperature differences between the samples, whilst within the study published in 2007, the infrared emittance of the samples was also measured with the use of an "emissometer", while the spectral reflectance of the samples was measured using a UV/VIS/NIR spectro-photometer. Yet again, the reported results do not deliver definite material specific information but solely comparisons.

Hagishima and Tanimoto (2003) made field measurements for estimating the convective heat transfer coefficient at building surfaces, being defined as the quotient of the convection heat flux [Wm^{-2}] and the temperature difference between air and surface. The material specificity was not studied, but mainly the dependence on wind velocity. Generally, the variation of the results was quite large.

In view of these uncertainties, it appeared appropriate, instead of delicately measuring the reflected radiation, applying a thermal method with respect to the substrate directly delivering the absorbance coefficient, while the complementary reflectance coefficient could be calculated, according to the relation $\alpha_s = 1 - \beta_s$. As a consequence, the heat capacity of the substrate (or the appropriate areal-specific thermal admittance [Jm^{-2}K^{-1}]), will be relevant. Moreover, a simultaneous heat-transfer between the substrate and the adjacent atmosphere-layer is to be expected insofar the sample gets warmer, reaching a limiting temperature where the warming-up rate is equal to the heat-emission rate. For fulfilling the empirical requirement of the investigation and thus excluding the hereof hypothetical relation of Stefan-Boltzmann, the cooling-down process should have to be studied empirically within separate experiments. Astonishingly, such a laboratory-like method with well-defined boundary conditions has not been presented, yet. The only known being roughly relevant seems that one described by Schwerdtfeger (1976), using a simple apparatus consisting of aluminium disks being set into insulating Styrofoam-blocks and laterally equipped with Hg-thermometers. Since they are cooled by an electric blower during the solar insolation, the influence of air convection is maximized instead of minimized. Moreover, this method affects only limiting, that is, stagnation conditions.

Summarizing it may be stated, firstly, that commonly no distinction is made between the notation "albedo" as a relative term, and the notation "solar reflection coefficient" as an absolute term, although it would be meaningful. Secondly, the indirect determination of the solar absorption coefficient β_s by determining the solar reflection coefficient α_s is delicate suggesting its direct determination. Thirdly, any hitherto applied thermic measuring methods implicated solely limiting temperatures without delivering the basis for a mathematical description of the temporal course of the heating-up and the cooling-down process. Moreover, they mostly were disturbed by uncontrollable influences of the surroundings, exhibiting rather field-like than laboratory-like conditions. All in all, in spite of the great amount of investigations and of the great efforts which have been expended yet, there is still no method available which yields more than relative values instead of reliable and well-defined ones, and which allows the precise modelling of the elementary process which occurs when sunlight comes upon a solid opaque surface.

OUTLINE OF THE PRESENT APPROACH

Within the present approach, not the reflected but the absorbed radiation is determined, namely by measuring the temperature courses of coloured quadratic plates (10 × 10 cm, usually 20 mm thick) with a known thermal specification when sunlight of a known intensity comes vertically onto these plates. They are embedded in Styrofoam, and covered with a thin transparent foil acting as an outer window to minimize erratic cooling by atmospheric turbulence. Thereby, the colours as well as the plate material are varied (aluminium, wood, brick and stone). As a reference material, aluminium is used being optimal due to its high heat conductivity and high heat capacity leading to a low heating rate and a homogeneous heat distribution. For enabling a correct orientation, the plate modules are positioned on an adjustable carrier. During the heating time of preferably 30 min, the equilibrium temperature was normally not reached, but the heating-rate could easily be determined by graphically assessing the initial slope.

For studying the cooling down behaviour, separate measurements have been made with preheated plates in a darkened room, the results being mathematically analysed. Hence, this method is solely based on thermal measurements using Hg-thermometers but omitting electronic instruments, except a "solarmeter" for measuring the intensity of the incident light during the warming-up process. If certain boundary conditions are fulfilled (constant atmospheric temperature, relatively thin plates and high thermal conductivity), the cooling-down process can be exactly expressed by a mathematical equation. Moreover, a stringent mathematical combination of the warming-up and the cooling-down process is feasible allowing to model the temporal energy transfer occurring between a solid surface layer and the contiguous air, and thus to study the influence of the colour and of the thermal admittance of the plate, as well as the temporal course of the temperature up to its limiting value.

The clearing of the relevant colour dependent termini is of special importance whereby partly novel designations and definitions are introduced. In particular, as initially mentioned, it is proposed distinguishing between the (relative) surface albedo a_s being colour dependent and related to a white surface exhibiting an albedo of 1, and the solar reflection coefficient α_s being related to the total energy flux of the incident light, and being coupled to the solar absorption coefficient β_s by the relation $\alpha_s = 1 - \beta_s$. Furthermore, the term solar colour factor b_s is introduced amounting the ratio between the solar absorption coefficients of the plates with the relevant colour and the white colour, or, easier, the ratio between the respective heat absorption rates.

Finally, some comparing albedo-measurements were made using a light-meter being directed towards wooden boards which have been coloured alike the original
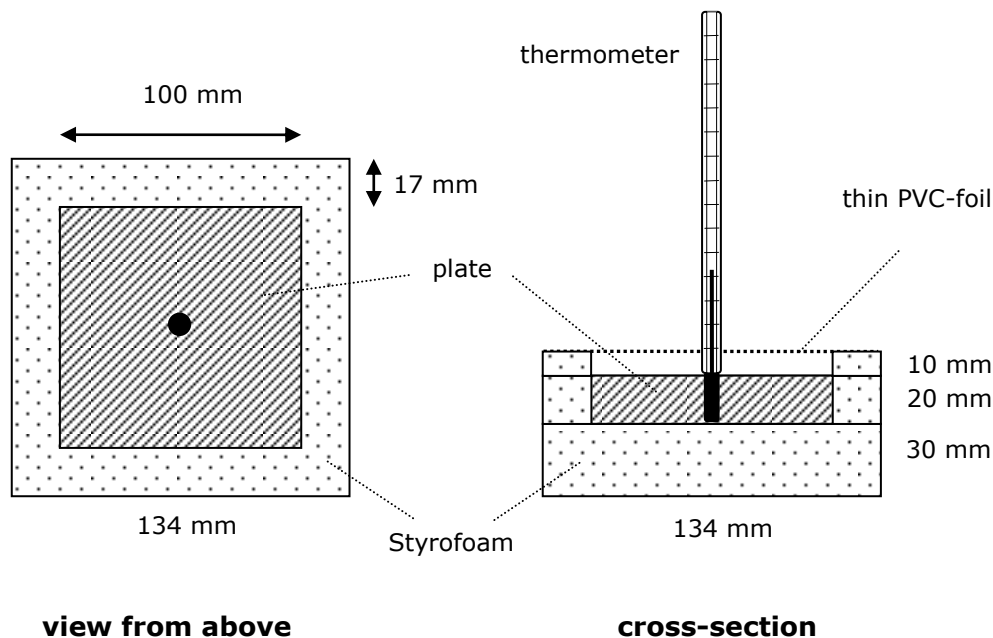
view from above   **cross-section**

Figure 1. Plate embedded into Styrofoam.

plates, a white plate serving as the reference.

EQUIPMENT, PROCEDURE AND MATERIALS

The warming-up experiments were carried out using small coloured quadratic plates (10×10 cm^{-2} and about 20 mm thick) from different materials (aluminium, wood, brick and stone) when sunlight of a known intensity (approx. 1000 Wm^{-2}) was coming vertically onto these plates (that is, perpendicular to the plates). Each plate was equipped with a Hg glass tube thermometer being inserted in centrally provided holes, and embedded in Styrofoam being covered with a thin transparent PVC-foil (0.07 mm) acting as an outer window, as schematized in Figure 1. The vertical positioning of the thermometer facilitated controlling the perpendicular arrangement of the module by regarding its shadow. However, in some appropriate cases the thermometer was attached laterally. At plate-materials with a low thermal conductivity (e.g. from brick or, in particular, from wood), the additional insertion of an aluminium foil into the thermometer holes was advantageous to enhance the thermal distribution.

Using a suitable panel comprising the plate modules and being directed by a mounting on a monopod at back, up to six measurements could be made simultaneously, as shown in Figure 2. The direction of the sun irradiation was determined by an aluminium tube being adjustably mounted on a tripod and measured by a goniometer. Prior to the experiment, all the modules were covered with aluminium-mirrored foils, avoiding a premature warming-up, and being removed at intervals of 10 s thereby starting the process. The temperature readings were made every 5 min. During the experiment lasting normally 30 min, the sky had to be cloud-free, and the modules were currently adjusted to the irradiation direction by stepwise revolving the padding on which the equipment has been established. The irradiation intensity was measured by a certified KIMO Solarmeter SL 100. The solar experiments have been made on a balcony in Glattbrugg (near Zurich/Switzerland, about 450 m above sea level) during several summer days, and preferably early in the afternoon. The atmospheric pressure was between 960 and 980 hPa, and the relative humidity between 50 and 60%.

The cooling-down experiments were made in a partly darkened room with a known ambient temperature between 20 and 25°C using the same modules. However, they were carried out partly, that is, bit by bit. Initially, each plate was heated in an oven up to a temperature above 60°C, and the start of the experiment was given when the temperature of the plate had reached 60.0°C. Afterwards, temperature readings were made at regular intervals, for aluminium of 15 min, and for wood or brick of 5 min (since the latter ones cooled down more rapidly).

The relevant features of the applied materials are listed in the Table 1. The brick-plates were sawed out from fresh red brick-pieces (being not weathered), and the (single) stone-plate was also sawed out from a natural granite boulder found in the Alps. The mass variance of the plates was minimal. The densities of spruce-wood, brick and the granite-stone plates were determined using the usual water buoyance method. The heat capacity of spruce-wood was determined using a calorimeter. The other values, being not very reliable and thus enclosed in brackets, are taken from literature.

The following colours have been applied (being not specified more precisely): white (wh), bright brown (lb), vanilla (va), bright blue (bl), bright green (gr), brick-red (re), dark brown (db), and black (bk).

RESULTS AND INTERPRETATIONS

Solar warming-up experiments

The primary experiments were made with two series of six colours using plates from aluminium and spruce-wood. The results are displayed in Figures 3 and 4. The warming-up rates, expressed in grades per time (minutes

Figure 2. Panel comprising six modules.

Table 1. Relevant features of the applied materials.

Type	Thickness [mm]	Mass (middle) [g]	Density [gcm^{-3}]	Specific heat capacity [Jg^{-1}K^{-1}]	Total heat capacity [JK^{-1}]	Heat conductivity [Wm^{-1}K^{-1}]
Aluminium (al)	20.0	537.5	2.70	0.902	485	236
Wood (wo)	17.5	80.5	0.50	1.83	147	(0.1-0.2)
Brick (br)	14.5	245	2.06	(0.84)	(206)	(0.5-1.4)
Stone (st)	20.5	527.5	2.60	(0.79)	(417)	(2.8)

or seconds), were determined by graphically evaluating the initial (linear) slope.

Regarding these figures, firstly it is salient that the warming-up rates are much larger for wood than for aluminium. Secondly, the relative courses of the colour dependent rates are quite similar in both cases, the dark brown one being nearly equal to the black one, and the light green one being considerably high. And thirdly, in particular with wood and with dark colours, the rate courses were not linear all the more the temperature rose. A similar order is evident in the case of brick plates (Figure 5), also exhibiting high warming-up rates, whereby partly other colours were applied.

Formally, the initial warming-up rate is determined by the irradiation density of the sunlight, the solar absorption coefficient of the relevant colour, and the thermal admittance of the plate. Within the initial linear range, the resulting temperature is given by

$$\frac{T - T_0}{t} = \Phi \cdot \beta_s / C_A \qquad (4)$$

where T = temperature of the plate [K] or [°C], T_0 = starting temperature of the plate [K] or [°C], t = time [s], Φ = irradiation density on the surface [Wm^{-2}] where 1 W
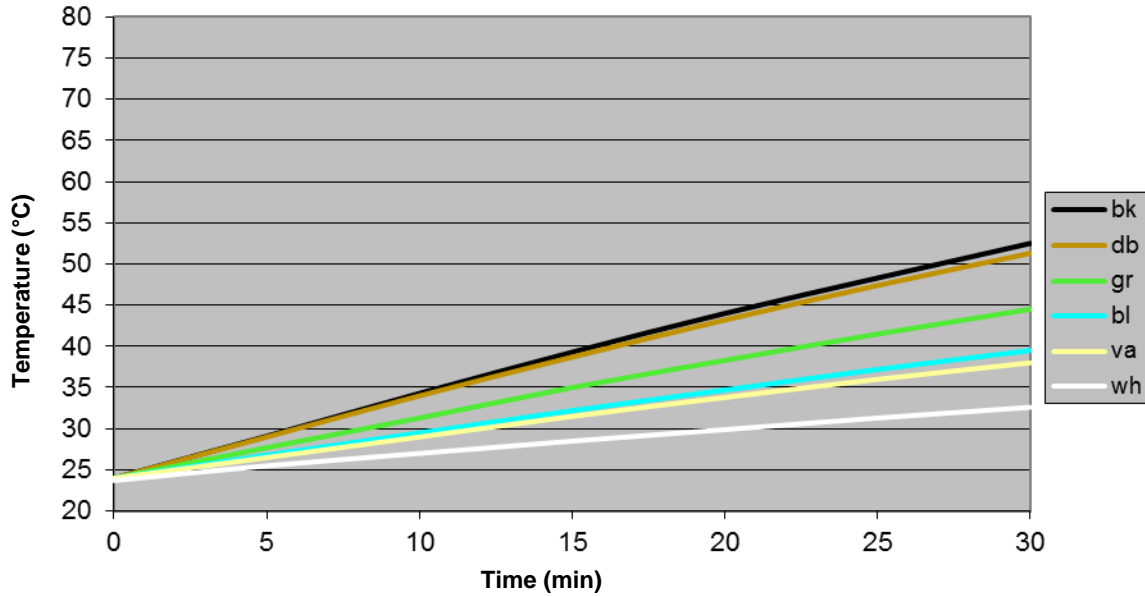
Figure 3. Warming-up of aluminium at 1040 Wm^{-2} 2013-09-04, 12:58 h. Initial slopes [°/min]: wh 0.31 / va 0.52 / bl 0.58 / gr 0.77 / db 1.02 / bk 1.08.
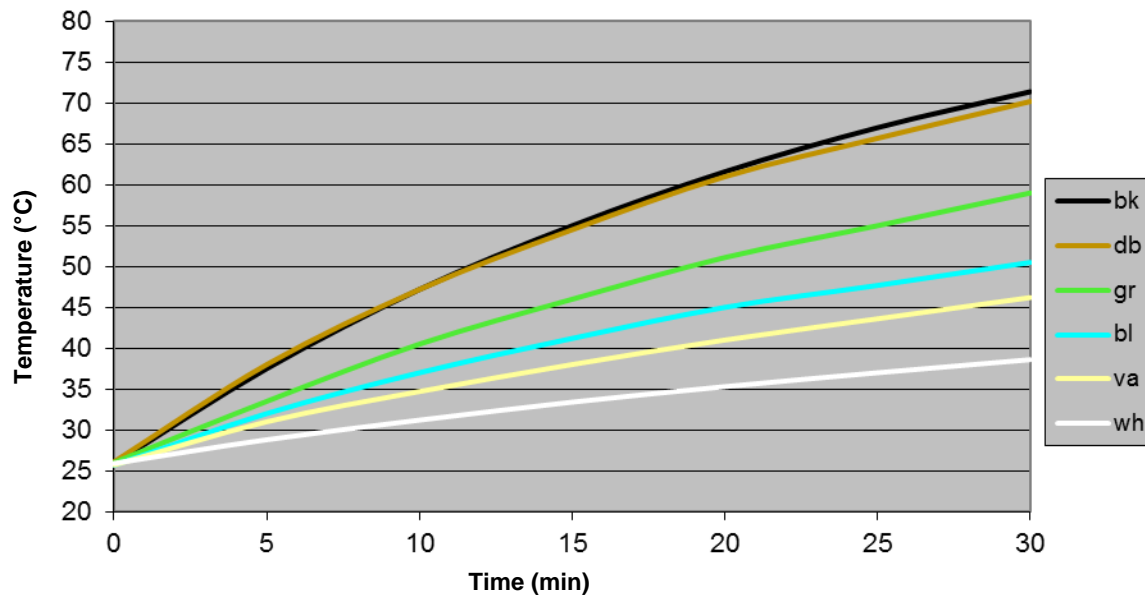
Figure 4. Warming-up of wood at 970 Wm^{-2} 2013-09-06, 12:43 h. Initial slopes [°/min]: wh 0.60 / va 1.02 / bl 1.20 / gr 1.57 / db 2.35 / bk 2.45.

= 1 Js^{-1}, β_s = solar absorption coefficient, $C_A = c_m \cdot \rho \cdot d \cdot 10^4$ = thermal admittance of the plate [Jm^{-2}K^{-1}], c_m = mass specific heat capacity of the plate material [Jg^{-1}K^{-1}], ρ = density of the plate material [gcm^{-3}], and d = thickness of the plate [cm].

The evident differences of the warming-up rates between aluminium, on one hand, and wood as well as brick, on the other hand, may be basically explained by the differences of their thermal admittances, whereas the deviation of the linearity at the ends of the curves is due to the thermal radiation being emitted by the plates insofar as the temperature difference to the environment increases.

Inserting the values given in Table 1, the following thermal admittances are obtained (in Jm^{-2}K^{-1}): aluminium 48'700, stone 41'700, brick 20'600, and wood 14'700.
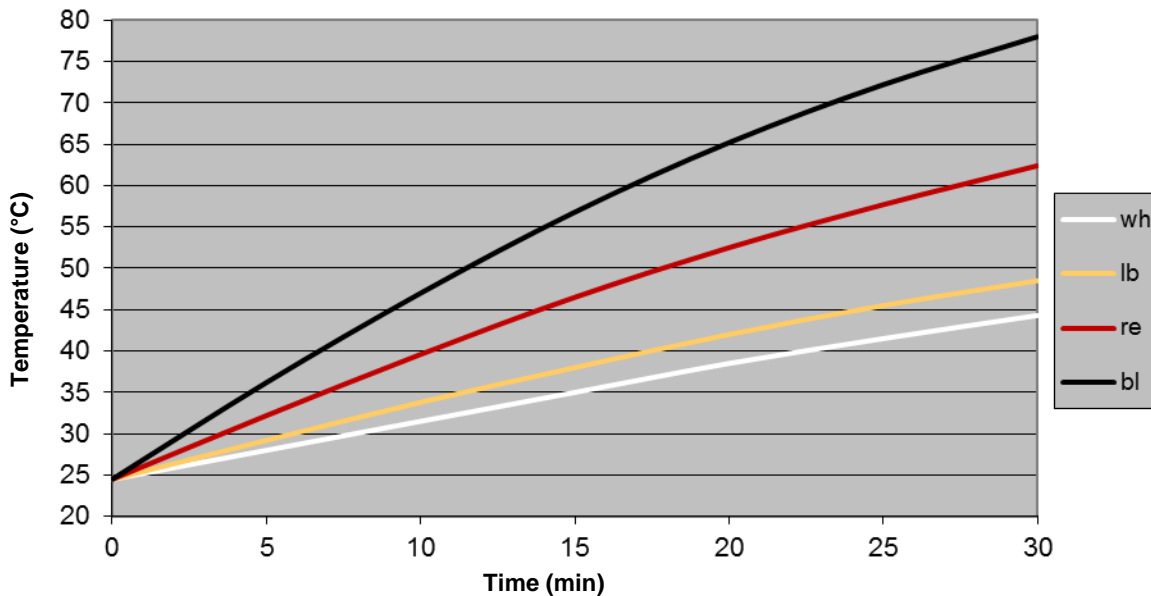
Figure 5. Warming-up of brick plates at 1050 Wm^{-2} 2013-09-04, 14:52 h. Initial slopes [°/min]: wh 0.70 / lb 0.98 / re 1.61 / bk 2.37.
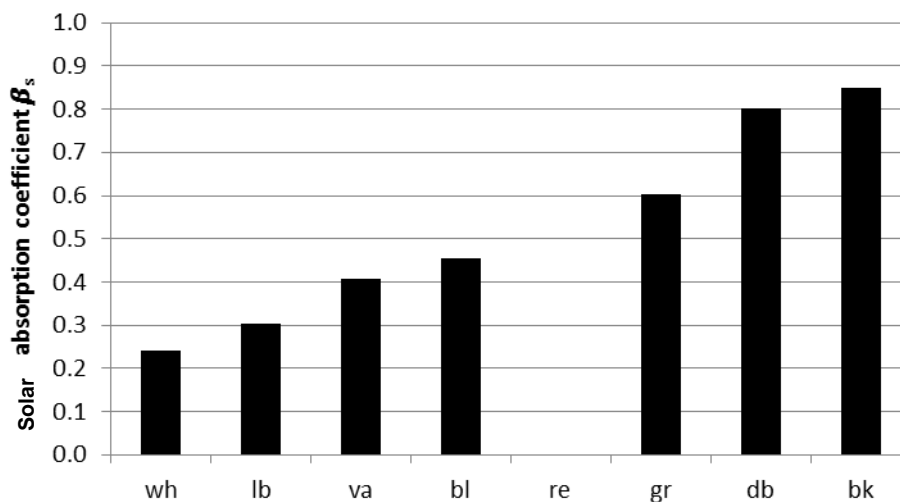

Figure 6. Solar absorption coefficients β_s on aluminium (colour code p. 8).

Inserting the aforementioned thermal admittances and using the expression of the slope given in formula (Equation 4), the (colour dependent) solar absorption coefficients β_s and, as a consequence, the solar reflection coefficients $\alpha_s = 1 - \beta_s$ can be calculated yielding for aluminium plates the values being plotted in Figures 6 and 7, and being best suited as standards due to their high thermal admittance as well as their thermal conductivities.

Hence, the white solar absorption coefficient is 0.24, and the black absorption coefficient 0.85, corresponding to solar reflection coefficients of 0.76 and 0.15.

Using the values of the solar reflection coefficients given in Figure 7, and relating them on the white surface assuming it as 1.0, for the real surface albedos a_s you get the values of Figure 8, the black colour exhibiting a value of 0.20.

Applying that procedure and using the averages of at least two differently measured values being normalized to the intensity of 1000 Wm^{-2}, the following radiate colour factors b_s have been found being compared in Figure 9, in the case of aluminium the black colour factor exhibiting the value of approximately 3.5.

However, comparing the warming-up rates at the different materials, there emerges the inconsistency that
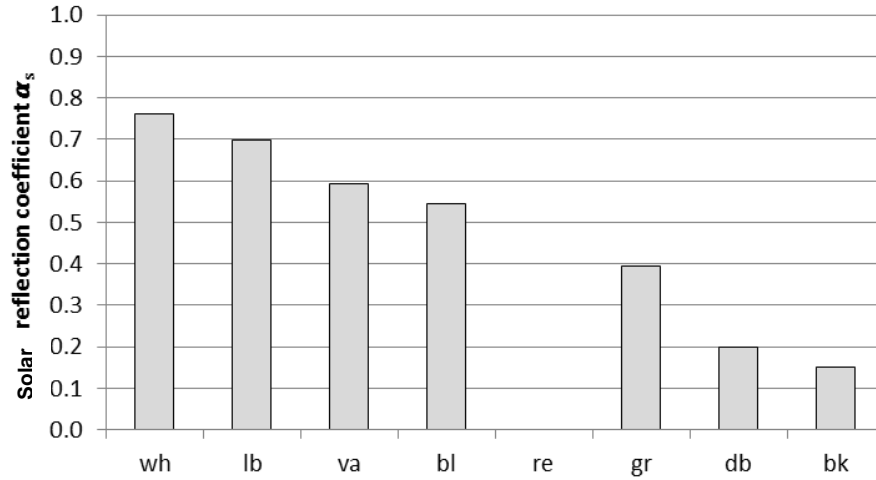
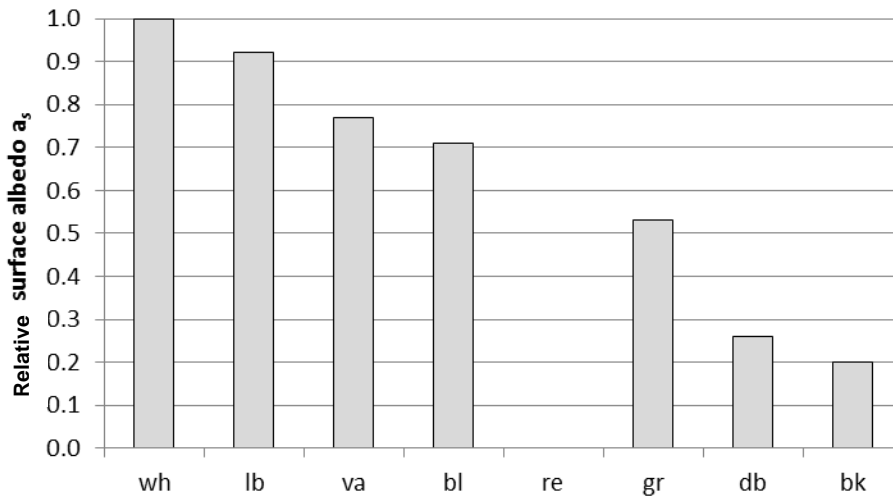**Figure 7.** Solar reflection coefficients α_s on aluminium (colour code p. 8).

Figure 8. Relative surface albedos a_s on aluminium (colour code p. 8).
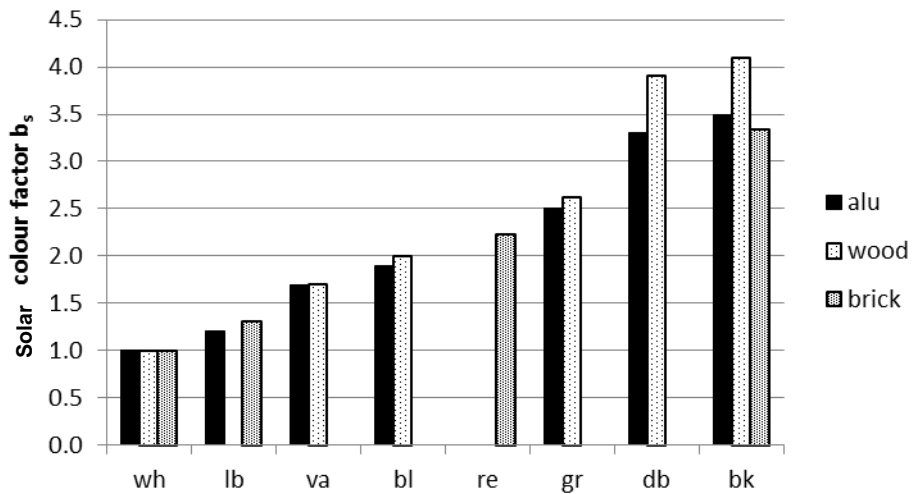

Figure 9. Solar colour factors b_s on different materials (colour code p. 8).
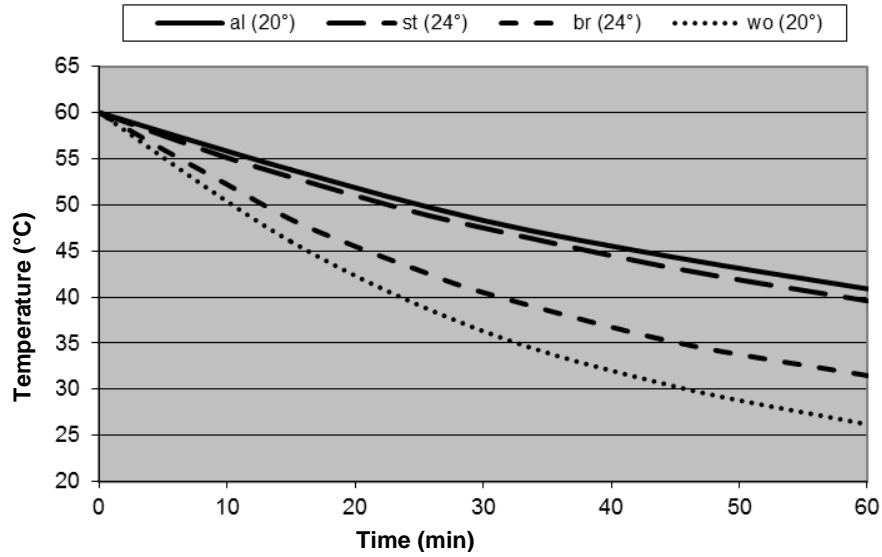
Figure 10. Cooling-down of different materials, with foil (in brackets: ambient temperature).
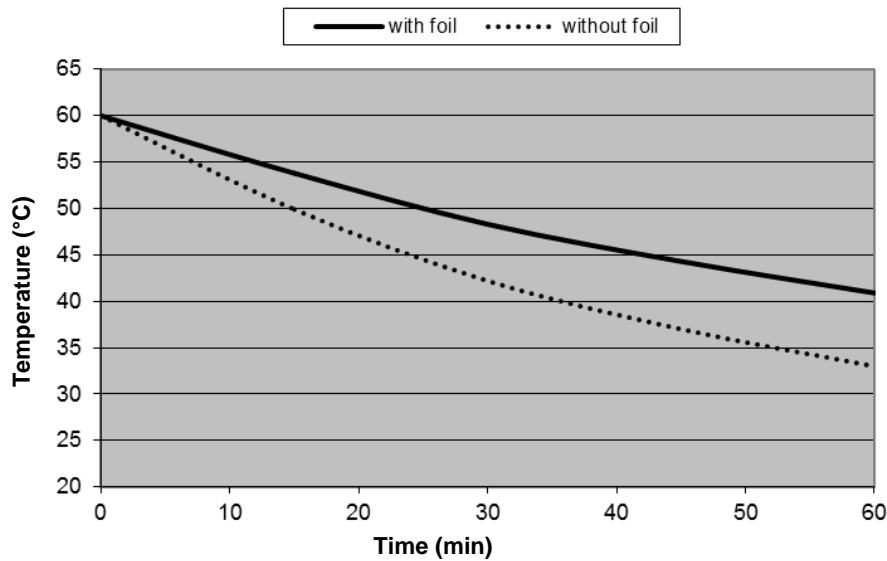

Figure 11. The isolating effect of a foil for aluminium.

for each colour, e.g. for black, the warming-up rates were not just inversely proportional to the thermal admittances; that is, for wood the warming-up rate was considerably smaller than theoretically expected, namely about 0.60 times as large.

For brick, this factor was less small, namely 0.91, while for granite-stone it was 0.95. But that may be explained by the low heat-conductivity, particularly of wood, leading to a vertical temperature gradient within the plate accompanied by an enhanced surface temperature compared to the measured average one, particularly with dark surfaces.

Cooling-down experiments

The procedure has already been described earlier. The primary observation was that, apparently contrary to Kirchhoff's Radiation Law, the long-wave radiate emission was completely independent of the colour of the plate but dependent on the material, as evident from Figure 10. Moreover, the ordinarily applied thin transparent PVC-foil (0.07 mm) had a considerable influence on the cooling down rate, as evident from Figure 11. The temporal course was not linear but converging to an equilibrium temperature being equivalent to the ambient room
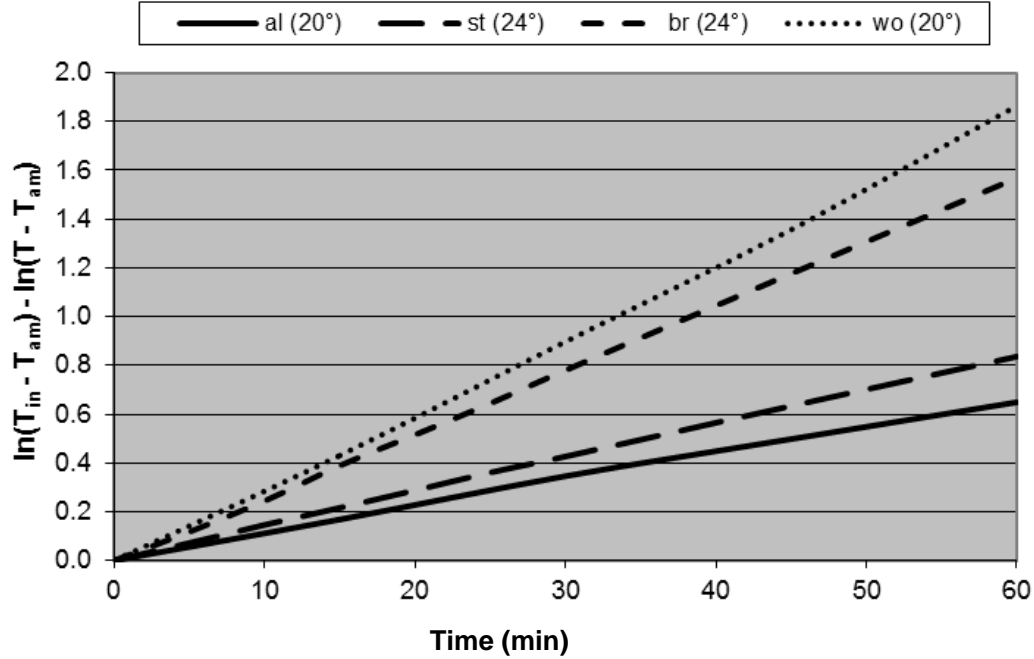
Figure 12. Logarithmic plots of the cooling-down data, with foil (in brackets: ambient temperature).

temperature. Thus for these experiments, differing from real natural conditions, the temperature of the ambient atmosphere was constant.

Assuming an interference of heat diffusion and of radiation and thus using, as explained in the introduction, Newton's Law (3) instead of the modified Stefan-Boltzmann Law (2), a mathematical modelling may start from the following differential approach, valid for a given plate area:

$$-m \cdot c_m \frac{dT}{dt} = B \cdot A(T - T_{am}) \qquad (5)$$

wherein t = time, T = (surface) temperature of the plate, T_{am} = ambient (room) temperature, B = heat transfer coefficient [Wm^{-2}K^{-1}], and A = surface area [m^2]. The further abbreviations are listed together with formula (Equation 4). This differential equation can be resolved as follows:

$$T = T_{am} + (T_{in} - T_{am}) \cdot e^{-\frac{B \cdot A}{m \cdot c_m}t} \qquad (6)$$

Where in T_{in} = initial (surface) temperature of the plate.

Instead of the absolute temperatures, given in °K, the °C values may be used. For determining the heat transfer coefficient B from experimental data, the logarithmic form of Equation 6 may be used, delivering a linear plot:

$$\ln(T_{in} - T_{am}) - \ln(T - T_{am}) = \frac{B \cdot A}{m \cdot c_m}t \qquad (7)$$

Inserting the heat capacity values listed in the Table 1, the evaluation of the logarithmic plots of Figure 12 yields the following values for the heat transfer coefficients B [Wm^{-2}K^{-1}], with foil:
Aluminium (al): 8.8; Stone (st): 9.7; Brick (br): 9.0; Wood (wo): 7.4.

The relatively small deviations for stone and for brick compared to the value for aluminium, being the most reliable one, may be due to inaccuracies of the heat capacity values. Moreover, it may be considered that the measurements for stone and for brick have been made at another time and on another day of the year; hence, the (room) atmosphere could have been slightly deviating. However, the greater deviation of the value for wood is probably due to its reduced heat conductivity, but being smaller than in the case of the warming-up experiment (accordance factor: 0.84 compared to 0.60, cf. chapter 4.1., p. 13 beneath). Overall, the results are enough satisfying and suggest a general heat transfer coefficient of approximately 9 Wm^{-2}K^{-1}. In the case of the absence of a foil, the heat transfer coefficient increased by the factor 1.7, being determined analogously using the results of Figure 11. Thus, for flat plates, the heat transfer coefficient comes up to more than 15 Wm^{-2}K^{-1} even when the atmosphere is quiet, that is, when there is no significant turbulence. This means that, at a temperature difference of 10°, the heat flux at the air/ground interface

would be 150 Wm^{-2}, that value being in good accordance with the values of Asaeda et al. (1996) for pavements, as cited incipiently.

However, the theoretical value of 6 Wm^{-2}K^{-1} resulting from the modified and simplified Stefan-Boltzmann Law (cf. 1. Introduction, formula (Equation 2)) is much lower than the here measured values even in the presence of a foil, meaning that the apparent heat transfer coefficient is significantly larger than the theoretical one predicted by the modified Stefan-Boltzmann Law. This fact is certainly due to an additional heat transfer by heat diffusion through the air. Moreover, no evidence could be found for the existence of an additional emissivity coefficient ε being commonly implemented in the modified Stefan-Boltzmann relation (Equation 2), implying an even smaller heat transfer since it is principally assumed to be smaller than 1. But in spite of the uncertainties due to the variable atmospheric conditions, it may be stated that, when the heat conductivity within the solid surface layer is sufficient, the apparent heat transfer coefficient is usually at least two and a half times as large as the modified Stefan-Boltzmann Law predicts. But when the material specific heat conductivity is low compared to the layer-thickness, it certainly gets rate-determining distorting that regularity.

THE COMBINATION OF THE WARMING-UP AND THE COOLING-DOWN PROCESS

When a plate is exposed to solar irradiation of a constant intensity, its temperature initially rises linearly but, in the course of time, a counter reaction occurs due to the increasing thermal emission, leading to a decrease of the warming-up rate until an equilibrium temperature is reached. Within the foregoing chapter, the two processes were studied separately, the first one at the starting range where the temperature increase was nearly linear, and the second one separately in a darkened room where no simultaneous warming-up occurred. Now the two effects shall be mathematically combined to a time-temperature-curve disclosing the overall process.

Thereto, the warming up rate $\dot{T}_\uparrow$ may be expressed by differentiation of Equation 4:

$$\dot{T}_\uparrow = \partial T_\uparrow / \partial t = \Phi(1 - \alpha_s)/C_A = k_1 \qquad (8)$$

On the other hand, the cooling down rate $\dot{T}_\downarrow$ is delivered by Equation 5:

$$\dot{T}_\downarrow = \frac{dT_\downarrow}{dt} = -\frac{B \cdot A}{m \cdot c_m}(T - T_{am}) = -k_2(T - T_{am}) \qquad (9)$$

where the two constants k_1 and k_2 have been introduced for the sake of convenience.

The total temperature rate is given by the sum of the two single temperature rates:

$$\dot{T} = \dot{T}_\uparrow + \dot{T}_\downarrow = k_1 - k_2(T - T_{am}) = k_1 + k_2 T_{am} - k_2 T \qquad (10)$$

This differential Equation 10 is resolvable yielding the explicit form (Equation 11):

$$T = T_{am} + \frac{k_1}{k_2}\left(1 - e^{-k_2 t}\right) = T_{am} + \frac{\Phi(1 - \alpha_s)}{B}\left(1 - e^{-\frac{B \cdot A}{m \cdot c_m}t}\right) \qquad (11)$$

When $t = \infty$, T has reached a limes being calculated by Equation 12:

$$T_{\lim} = T_{am} + \frac{\Phi(1 - \alpha_s)}{B} \qquad (12)$$

Hence, according to formula (Equation 12), the limiting temperature is independent of the thermal admittance or the heat capacity, respectively, but solely dependent on the irradiation density Φ, the solar reflection coefficient α_s, and the heat transfer coefficient B. E.g. in the case of the black aluminium plate, exhibiting a solar reflection coefficient of 0.15 and a heat transfer coefficient of 8.8 Wm^{-2}K^{-1} (in the presence of a cover-foil), and at a solar irradiation density of 1000 Wm^{-2}, the maximal temperature enhancement is approximately 95°(K or C), whilst in the case of the white aluminium plate, exhibiting a solar reflection coefficient of 0.76, the maximal temperature enhancement is approximately 27°(K or C). If the ambient temperature T_{am} is assumed to be 25°C, the resulting limiting temperatures are 120° (for the black plate) and 52°(for the white plate), respectively.

The Figures 13 and 14, being derived from Equation 11, illustrate the influences of the surface colour (black and white), the thermal admittance and the cover foil, solely inserting aluminium plates but being variously thick (20 mm or 10 mm). From Figure 13 (with B = 8.8 Wm^{-2}K^{-1}), it is evident that the limiting temperature for the black plates is considerably higher than for the white plates. But in the cases of the thinner plates, the processes are proceeding faster than in the case of the thicker plates, exhibiting a larger (twice as much) thermal admittance. In principle, the situation being outlined in Figure 14 (with B = 15 Wm^{-2}·K^{-1}) is similar, but the limiting temperatures are generally lower due to the absence of the cover foil leading to accelerated heat emission.

Analogously and for comparison, the temperature courses of differently coloured at aluminium-plates (Figure 15), as well as at brick-plates (Figure 16), may be calculated (with foil). These plots reveal that the heating-rates of the aluminium-plates are much smaller than those of the brick-plates, namely due to the larger thermal admittance, while the limiting temperatures are equal in both cases. And, as being already evident from
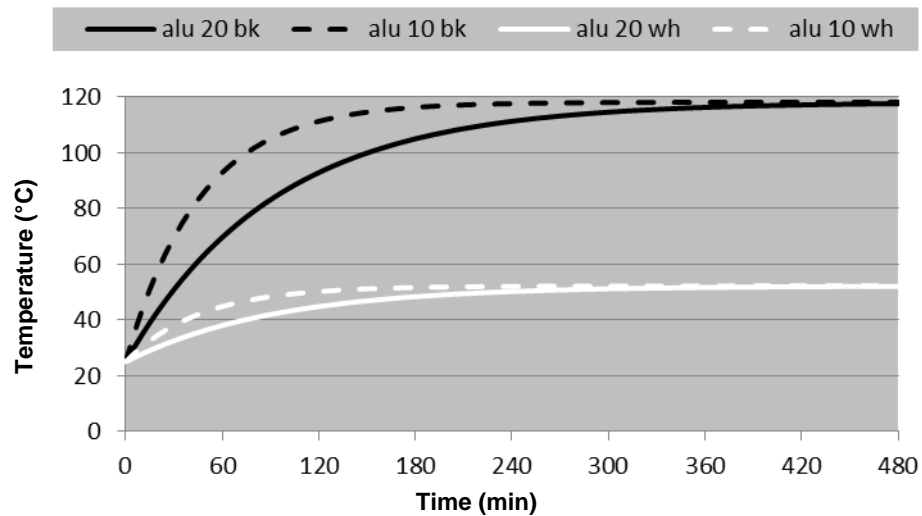
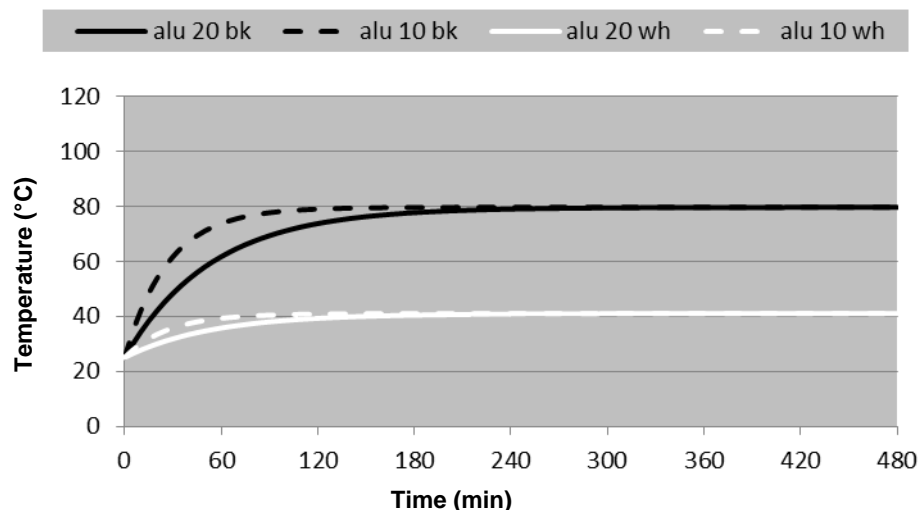**Figure 13.** Temperature courses with foil (at 1000 Wm^{-2}, calculated).

Figure 14. Temperature courses without foil (at 1000 Wm^{-2}, calculated).

the previous diagrams, the green colour implicates a relatively high limiting temperature due to its relatively low albedo or solar reflection coefficient, respectively.

In addition, the given formulas allow an exemplary lining-up of the warming-up and the subsequent cooling-down process. Comparing blackened stone and blackened brick, e.g., such a possible two-step combination is shown in Figure 17 where the warming-up curves are based on real measurements (at 1020 Wm^{-2}), and the cooling-down curves are calculated by formula (Equation 6) using the given material constants, assuming an ambient temperature of 24.5°C. Thereby it has to be remembered that the stone-plate was considerably thicker than the brick-plate (20.5 compared to 14.5 mm).

Conclusions

Due to the mathematical analysis of the diverse warming-up and cooling-down experiments, the following statements can be made: The warming-up rate of a solid plate depends on the intensity of the solar radiation, on the surface-colour of the plate and thus on its solar absorption coefficient, and on its thermal admittance being given by the heat capacity of the plate, its thickness and its density. On the other hand, the cooling-down rate depends on its temperature difference to the surroundings, on the thermal admittance of the plate, and on the heat-transfer coefficient but not on the surface-colour. Moreover, the heat-conductivity of the material may be relevant. Thereby, the heat-transfer coefficient
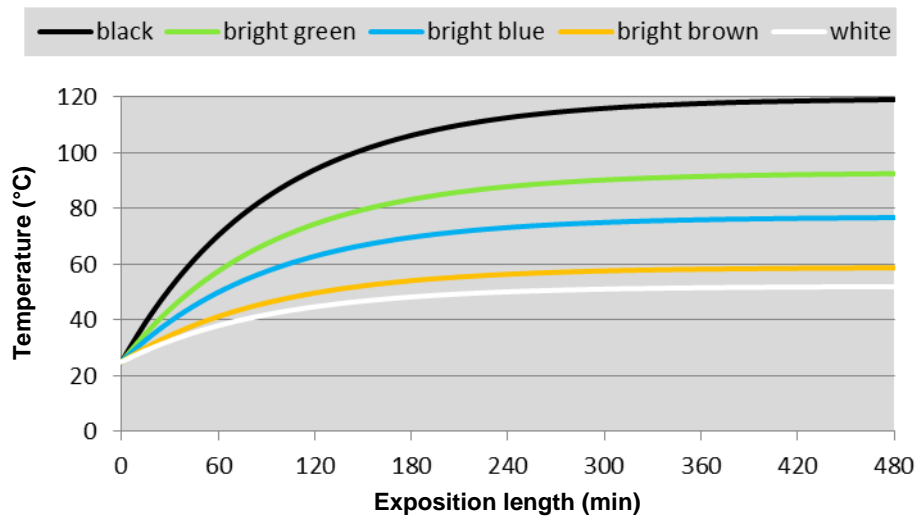
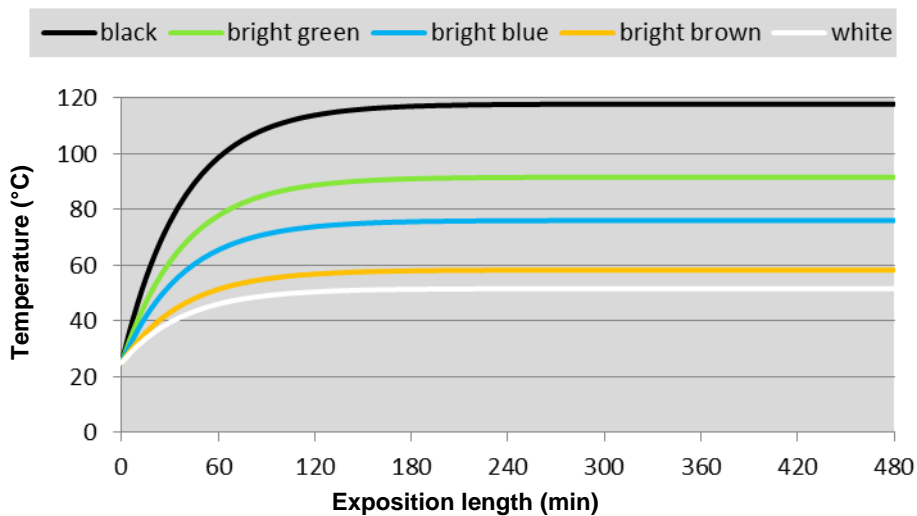**Figure 15.** Temperature courses at differently coloured aluminium-plates.

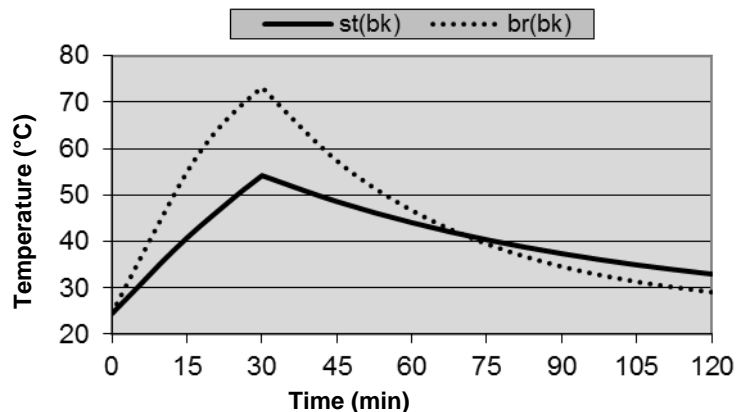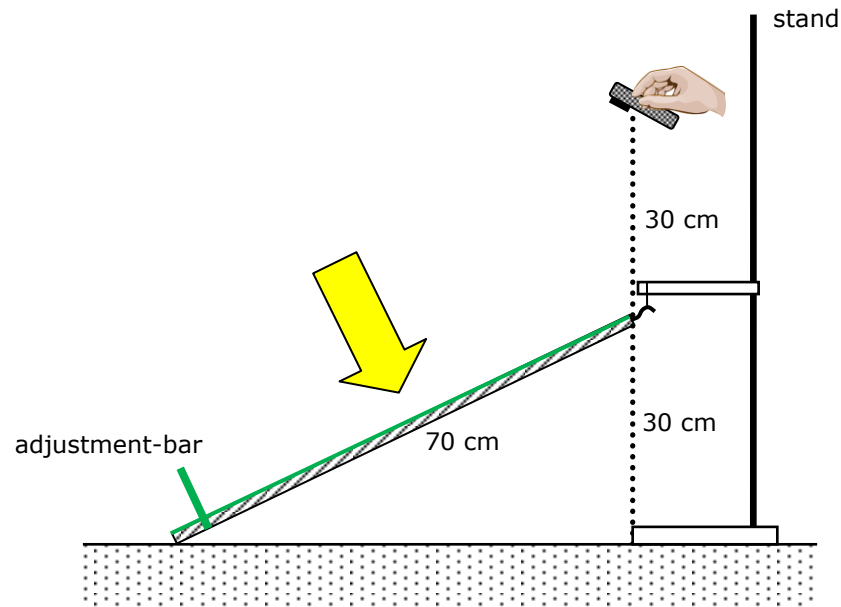**Figure 16.** Temperature courses at differently coloured brick-plates.

Figure 17. Two-step combination for stone and for brick.

Figure 18. Assembly for the albedo-measurement by a light-meter.

depends on the atmospheric conditions at the surface such as air-convection but apparently not on material features (except the thermal conductance), while the Stefan-Boltzmann Law appeared to be invalid under atmospheric conditions. The limiting temperature depends on the intensity of the solar radiation, on the surface-colour of the plate and thus on its solar absorption coefficient, on its thermal admittance, and on the heat-transfer coefficient. For these experiments, the atmospheric influences usually have been minimized by attaching a thin transparent foil providing an outer window. However, they are not quantized in such a way that they would enable a complete modelling of microclimates. The same is true with respect to the thermal conductance of the soil which has a considerable impact on microclimates.

Comparing reflection measurements by a light-meter

As herewith demonstrated, this caloric method permits a quite exact determination of the relevant key values, as well as a mathematic description of the basic processes. However, it requires an accurate preparation of well-defined materials and the availability of the convenient equipment, being thus not suitable for field-measurements. Moreover, its relation to the conventional method of measuring the reflected radiation has not been empirically proven. Therefore, finally an easy device shall be proposed exhibiting both requirements. However, instead of the pyranometer for measuring the reflected radiation operating in the range of 280 to 2800 nm as being recommended in the quoted ASTM Standard

E1918-06, a normal light-meter has been used, operating in the visible light range and being customary for photography and delivering the measured values in lux. Naturally, it would solely allow the determination of relative albedo-values, that is, being related to a white surface, but they may be compared with the albedo-values which have been evaluated by the caloric method. Since only the visible light is affected, temperature and wind are irrelevant. However, the measurements must always be made from the same position while the solar irradiance must be constant, which may be checked by a pyrheliometer. Nevertheless, as has already been objected, the precision of this method will presumably not be high, the more so as mirror-like reflection may occur.

Figure 18 shows an appropriate assembly for an albedo-measurement by a light-meter, using a white plastic-coated wooden board (60 × 70 cm) which has been painted with the respective colours. For this comparison, exactly the same colours were applied as for the previous experiments, namely white, vanilla, bright-green and black. For being able to adjust the board perpendicularly to the solar radiation by regarding the shadow, a small coloured bar (from aluminium) is attached near the bottom edge of the board. The inclination angle of the board depends on the time of the year and of the day, and was in this case about 25°. For avoiding the interference by its shadow, the light-meter has to be positioned laterally. As a light-meter, the Illuminometer i-346 from Sekonic was used, while the already used KIMO Solarmeter SL 100 served to measure the sunlight intensity.

The measurements have been made in July around two o'clock at a solar irradiance intensity of about 1040

Table 2. Method-comparison

Method	White	Vanilla	Bright-green	Black
Direct/Light-meter [lx]	58'500	15'000	28'000	47'500
Indirect (relative albedo)	1.000	0.770	0.530	0.200
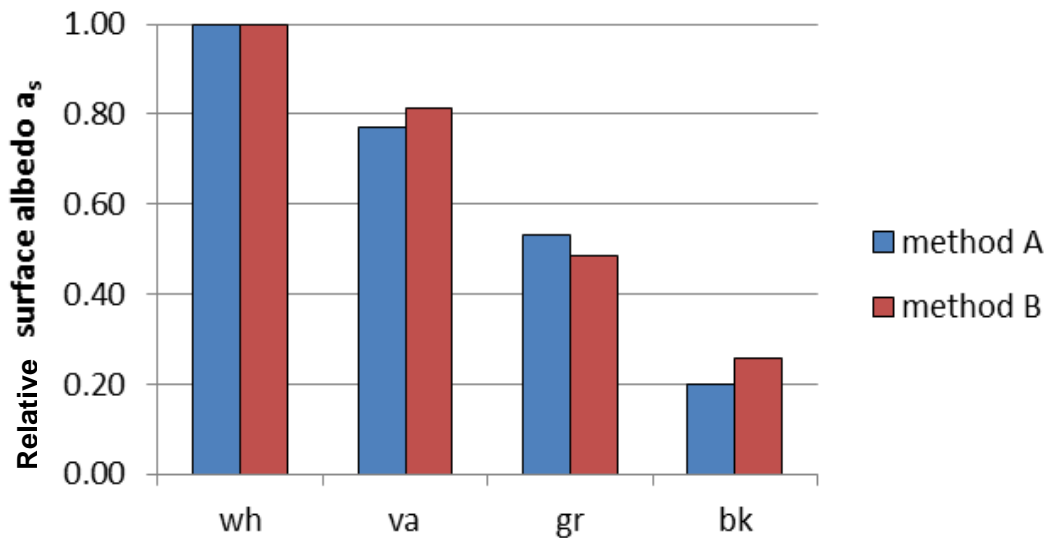
Figure 19. Method-comparison by means of the albedo-values.

Wm^{-2}. Thereby, the values in Table 2 were obtained, being compared with the values which have been earlier received by the caloric method:

Using these results, the albedo-values referring to the light-meter can easily be calculated delivering the comparison being illustrated in Figure 19, and revealing a remarkably good accordance of the two methods. However, the direct measurement delivers solely the relative values. For determining the absolute values concerning the solar reflection coefficient, a calibration on the basis of the caloric method is necessary.

Conflict of Interests

The author has declared no conflict of interests.

REFERENCES

Asaeda T, Thanh Ca V, Wake A (1996): Heat storage of pavement and its effect on the lower atmosphere, Atmos. Envir. 30:413-427.

Boltzmann L (1884). Ableitung des Stefan'schen Gesetzes betreffend die Abhängigkeit der Wärmestrahlung von der Temperatur aus der electromagnetischen Lichttheorie, Ann. Phys. Chem. 22:291-294.

Brady RF, Detrie T, Swiler D (1992). When black is white, Paint and Coatings Industry Magazine, January.

Coulson KL, Bouricins CM, Gray EL (1965). Optical Reflection Properties of Natural Surfaces, J. Geophys. Res. 70:4601-4611.

Coulson KL and Reynolds W (1971): The Spectral Reflectance of Natural Surfaces. J. Appl. Meteor. 10:1285-1295.

Coulson KL (1975). Solar and Terrestrial Radiation, Academic Press.

Doulos L, Santamouris M, Livada I (2004). Passive cooling of outdoor urban spaces. The role of materials, Solar Energy 77:231-249

Dulong MM, Petit AT (1817). Des Recherches sur la Mesure des Températures et sur les Lois de la communication de la chaleur; Annales de Chimie et de Physique, Ser. 2/7:225-264 ("Des Lois du Refroidissement"); ("Du Refroidissement dans l'air et dans les gaz") pp. 337-367.

Hagishima A, Tanimoto J (2003). Field measurements for estimating the convective heat transfer coefficient at building surfaces. Building Environ. 38:873-881.

Johnson GT, Watson ID (1984). The determination of view-factors in urban canyons. J. Clim. Appl. Meteorol. 23:329-335.

Levinson R, Berdahl P, Akbari H (2005). Solar spectral properties of pigments – Part I: model for deriving scattering and absorption coefficients from transmittance and reflectance measurements, Solar Energy Materials & Solar Cells Part II: survey of common colorants, Solar Energy Materials Solar Cells 89:351-389.

Levinson R, Akbari H, Berdahl P (2010). Measuring solar reflectance – Part I: Defining a metric that accurately predicts solar heat gain, Solar Energy 84:1717-1714; Part II: Review of practical methods, Solar

Energy 84:1745-1759.

Meschede D (2002). Gerthsen Physik, Springer-Verlag Berlin Heidelberg, 21. Aufl.

Pomerantz M, Akbari H, Berdahl P, Konopacki SJ, Taha H, Rosenfeld AH (1999). Reflective surfaces for cooler buildings and cities, Philosophical Magazine Part B 79(9):1457-1476.

Schwerdtfeger P (1976). Physical Principles of Micro-Meteorological Measurements, Developments in Atmospheric Science 6, Elsevier.

Stefan J (1879). Über die Beziehung zwischen der Wärmestrahlung und der Temperatur; Sitzungsberichte der mathematisch-naturwissenschaftlichen Classe der kaiserlichen Akademie der Wissenschaften 79:391-428.

Synnefa A, Santamouris M, Livada I (2006). A study of the thermal performance of reflective coatings for the urban environment, Solar Energy 80:968-981.

Synnefa A, Santamouris M, Apostolakis K (2007). On the development, optical properties and thermal performance of cool colored coatings for the urban environment, Solar Energy 81:488-497.

Visconti G (2001). Fundamentals of Physics and Chemistry of the Atmosphere, Springer-Verlag Berlin Heidelberg.

Zerlaut G (1989). Solar Radiation Instrumentation, Solar Resources, R. L. Hulstrom, ed., MIT Press, Cambridge, MA, pp. 173-308.